www.czasopisma.pan.pl PAN POLSKA AKADEMIA NAUK www.journals.pan.pl

Arch. Metall. Mater. **66** (2021), 4, 1007-1011

DOI: 10.24425/amm.2021.136415

YOUNG-CHUL YOON[1], SANG-GYU KIM[1], SANG-HYEOK LEE[1], BYOUNGCHUL HWANG[1*]

INFLUENCE OF Al, Cu AND Ni ADDITIONS ON MECHANICAL PROPERTIES OF HOT-ROLLED Fe-9Mn-0.2C MEDIUM-MANGANESE STEELS

The microstructure and mechanical properties of hot-rolled Fe-9Mn-0.2C medium-manganese steels with different Al, Cu, and Ni contents were investigated in this study. Based on the SEM, XRD, and EBSD analysis results, the microstructure was composed of martensite, band-type delta ferrite, and retained austenite phases depending on the Al, Cu, and Ni additions. The tensile and Charpy impact test results showed that the sole addition of Al reduced significantly impact toughness by the presence of delta-ferrite and the decrease of austenite stability although it increased yield strength. However, the combined addition of Al and Cu or Ni provided the best combination of high yield strength and good impact toughness because of solid solution strengthening and increased austenite stability.

Keywords: medium-manganese steel, hot-rolled, microstructure, strength, impact toughness

1. Introduction

Recently, the demand for eco-friendly energy sources such as liquefied natural gas (LNG) and hydrogen gas has been increased as environmental regulations become more restrictive. To date, austenitic stainless steels, 9% Ni steel, and high-manganese austenitic steels have been used as cryogenic ferrous alloys for the transport and storage of LNG [1-6]. However, all of these materials have some disadvantages, including relatively high prices, welding issues, and low design strength, among others. Medium-manganese steels with manganese contents between 3 and 12 wt.% can be considered as a promising material for cryogenic applications owing to their excellent mechanical properties combining high strength and ductility as well as good low-temperature impact toughness [7,8].

The mechanical properties and microstructure of the medium-manganese steels vary with their chemical composition, rolling condition, and heat treatments [9]. Although many researchers have attempted to understand a correlation between the microstructure and the mechanical properties [10-14], there are few studies on the influence of alloying elements on mechanical properties including impact toughness. In the present study, four kinds of Fe-9Mn-0.2C medium-manganese steels with different Al, Cu, and Ni contents were fabricated and the microstructure was characterized by scanning electron microscopy (SEM), X-ray diffraction (XRD), and electron back scatter diffraction (EBSD) analysis. The tensile and impact tests were also performed to correlate the microstructure with mechanical properties of Fe-9Mn-0.2C medium-manganese steels.

2. Experimental

Four kinds of Fe-9Mn-0.2C medium-manganese steels with 3 wt.% Al, 1.5 wt.% Cu, and Ni contents were made by a vacuum-induction melting method; the four steels are referred to as 'BASE', 'Al', 'AlCu', and 'AlNi' according to the single or combined additions of Al, Cu, and Ni. After an ingot was homogenized at a temperature exceeding 1,200°C, it was hot-rolled at temperatures more than 900 °C to a thickness of 15 mm and then cooled in the air to room temperature.

The longitudinal-short transverse (L-S) plane of the medium-manganese steel samples was mechanically polished and then electro-polished in a mixed solution of 90% glacial acetic acid (CH_3COOH) and 10% perchloric acid ($HClO_4$). The corresponding microstructures were observed by SEM (model: VEGA3, Tescan, Czechia) and EBSD (model: CrystAlign e-Flash^{HR}, Bruker, Germany). EBSD analysis data were processed

[1] SEOUL NATIONAL UNIVERSITY OF SCIENCE AND TECHNOLOGY, DEPARTMENT OF MATERIALS SCIENCE AND ENGINEERING, 232, GONGNEUNG-RO., NOWON-GU, SEOUL 01811, KOREA

* Corresponding author: bhwang@seoultech.ac.kr

using the TSL-OIM (ver. 5.3) program. The phases were identified by using an X-ray diffractometer (XRD; Bruker DE/D8 Advance, Bruker, Germany) with a Cu Kα target (λ = 1.5405 Å). The scanning rate and range used during the XRD analysis were 2° min^{-1} and 40°~100°, respectively.

Sub-sized sheet-type tensile specimens with a gauge diameter of 6.3 mm and a gauge length of 25.0 mm were taken along the rolling direction and then deformed at a strain rate of 0.001 s^{-1} at room temperature using a 10-ton capacity universal testing machine (model: UT-100E, MTDI, Korea) according to the ASTM E8 standard test method. The yield strength, tensile strength, total elongation, and work hardening index were obtained from the tensile stress-strain curves. For specimens exhibiting continuous yield behavior, the yield strength was defined as 0.2% offset at the stress-strain curve, and the work hardening index was calculated from the tensile stress-strain curve based on the Hollomon equation [15].

ASTM E23 standard Charpy V-notch specimens (size: 10 × 10 × 55 mm^3, orientation: transverse-longitudinal (T-L)) were tested at room temperature by a Charpy impact tester (model: DTI-603B, Daekyung Tech & Testers, Korea) with a capacity of 300 J. After the Charpy impact test, specimens were coated with Ni solution (5.5~6.5 g/L Ni density, 4.3~5.0 pH, and 85~92°C) in order to observe the cross-sectional area under fracture surfaces.

3. Results and discussion

The SEM micrographs of the BASE, Al, AlCu, and AlNi steels are given in Fig. 1. All steels contained lath-type ferrite and martensite. In particular, the Al, AlCu, and AlNi steels have band-type delta-ferrite whose fraction was 0.41±0.34, 2.22±0.69, and 3.31±0.68%, respectively. Fig. 2 shows XRD analysis results conducted to identify the microstructures of the medium-manganese steels more accurately. All steels were found to contain ferrite and martensite (α and α') peaks and the BASE steel exhibited some epsilon martensite (ε) with a hexagonal close-packed structure probably due to the low stacking fault energy [16]. However, austenite (γ) peaks appeared on the Al, AlCu, and AlNi steels because the addition of Al increased stacking fault energy and suppressed austenite transformation to martensite.

Fig. 3 provides EBSD analysis results of inverse pole figure (IPF), kernel-average misorientation (KAM), image quality (IQ), and phase maps for the Al, AlCu, and AlNi steels. The phases colored in red and green correspond to body-centered cubic (BCC) structure such as ferrite (α) and martensite (α'), and face-centered cubic (FCC) structure such as austenite (γ), respectively. The red and black lines represent low-angle boundaries with misorientation angles below 15° and high-angle boundaries with misorientation angles above 15°, respectively. The EBSD analysis indicated that a small amount of austenite was formed between the ferrite and martensite interface [17].

The tensile properties, Charpy impact absorbed energy, and Vickers hardness of the BASE, Al, AlCu, and AlNi steels, are presented in Table 1. The tensile stress-strain curves of all steels exhibited continuous yielding behavior without the occurrence of the serrated flow. In general, the medium-manganese steel annealed after cold rolling showed discontinuous yielding behavior because it had equiaxed ferrite with low dislocation density.

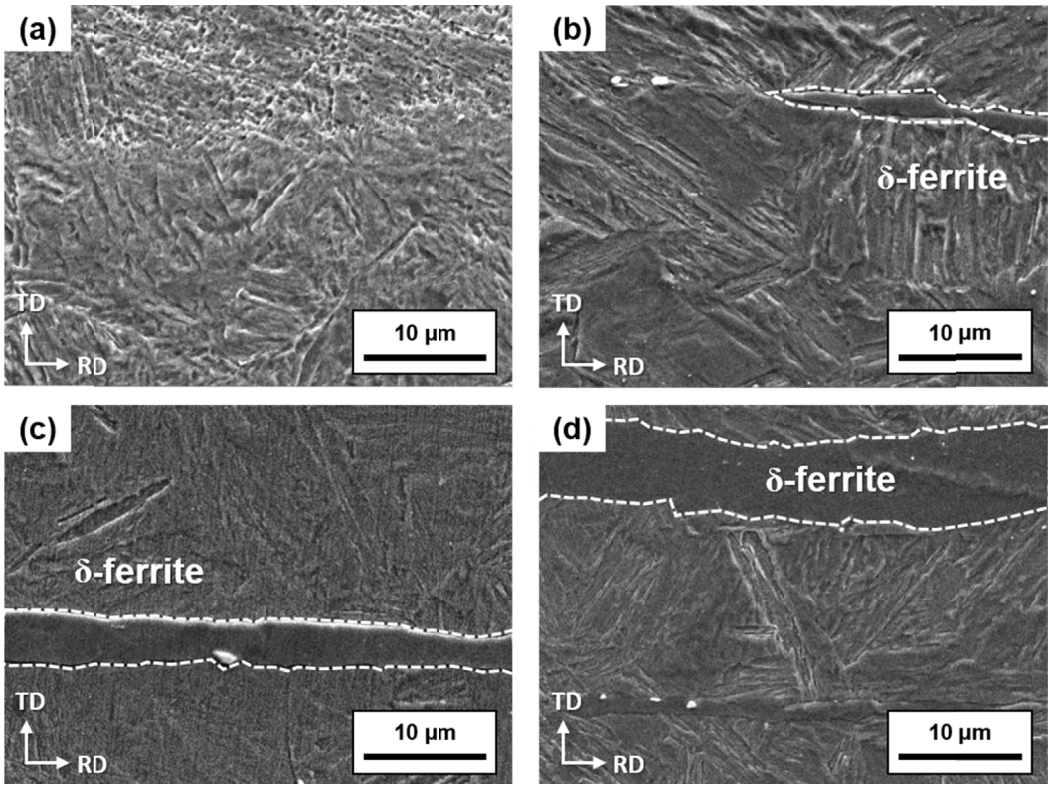

Fig. 1. SEM micrographs of the hot-rolled (a) BASE, (b) Al, (c) AlCu, (d) AlNi steels. Delta-ferrites (δ-ferrite) are marked in the micrographs

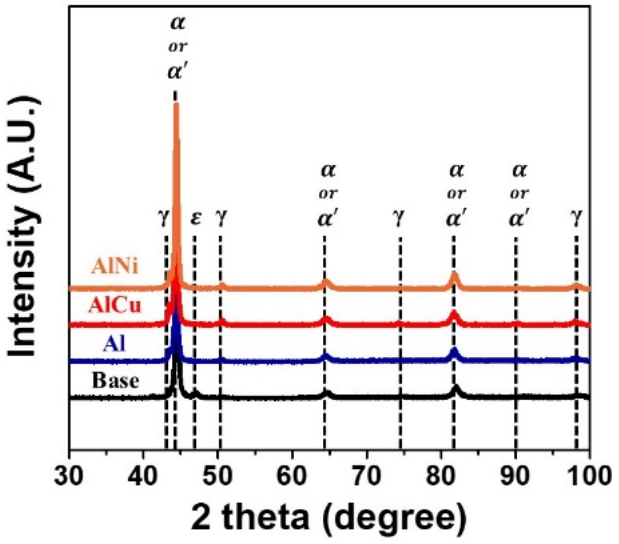

Fig. 2. X-ray diffraction (XRD) patterns of the hot-rolled Fe-9Mn-0.2C-0.5Si medium-manganese steels combined Al, Cu or Ni

However, the hot-rolled and annealed medium-manganese steel indicated continuous yield behavior because acicular ferrite and martensite that had high dislocation density were deformed at the same time [18]. With the addition of the alloying elements, the yield strength increases, but the tensile strength decreases for medium-manganese steels investigated in this study. The increase in the yield strength results from solid solution strengthening. However, the combined addition of alloying elements such as Al, Cu, and Ni to the BASE steel decreased the tensile strength as it promoted the formation of coarse delta-ferrite. The Charpy impact test results indicated all steels had relatively high absorbed energy levels over 20 J, and the Al steel had lower absorbed energy than the BASE steel, which can be explained by the formation of delta-ferrite associated with crack propagation. However, the AlCu and AlNi steels had similar absorbed energy comparable to the BASE steel because the addition of the austenite stabilizers such as Cu and Ni improves the retained austenite stability.

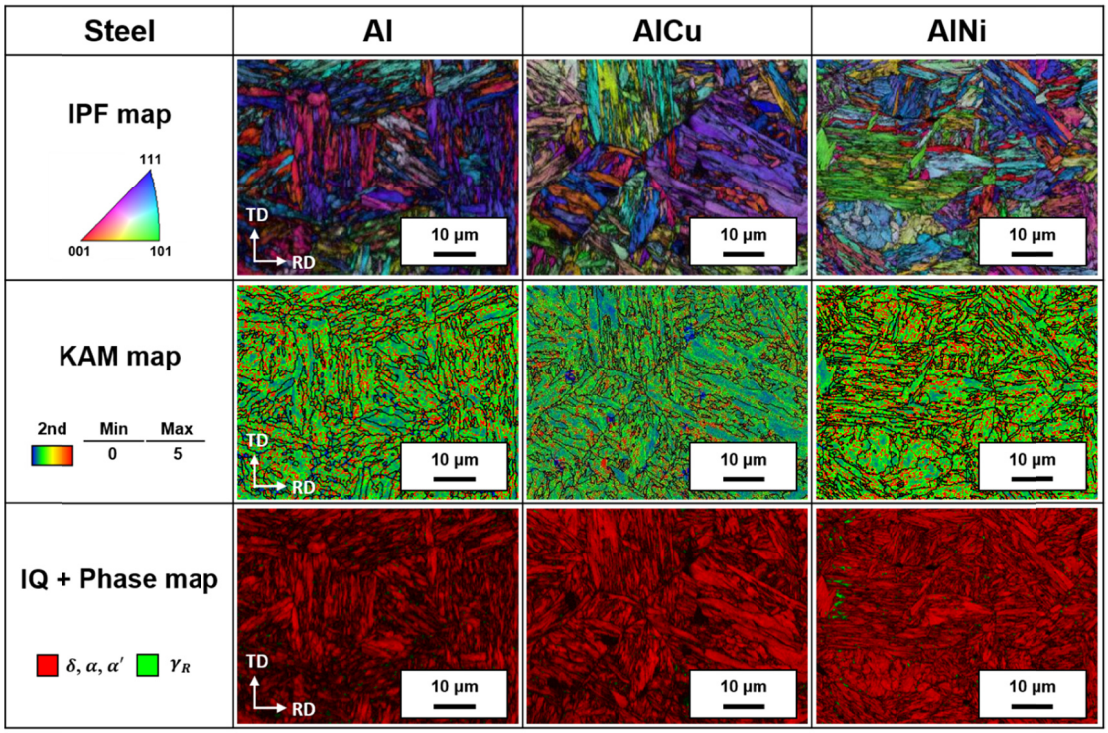

Fig. 3. EBSD analysis of the hot-rolled Fe-9Mn-0.2C-0.5Si medium-manganese steels combined Al, Cu or Ni. EBSD inverse pole figure (IPF), kernel average misorientation (KAM), image quality (IQ) and phase maps of the hot-rolled Al, AlCu, and AlNi steels showing ferrite (α,δ), martensite (α'), and retained austenite (γ_R)

TABLE 1

Mechanical properties of the hot-rolled Fe-9Mn-0.2C-0.5Si medium-manganese steels combined addition of Al and Ni or Cu

Steel	Tensile properties					Charpy impact absorbed energy, (J)	Vickers hardness, (Hv)*
	Yield strength, (MPa)	Tensile strength, (MPa)	Yield ratio	Total elongation, (%)	Work hardening exponent		
BASE	678	2,020	0.29	12.5	0.46	32.1	517
Al	921	1,610	0.57	12.1	0.25	20.9	468
AlCu	848	1,568	0.54	12.8	0.26	29.5	436
AlNi	770	1,432	0.54	12.5	0.28	28.2	417

* Vickers microhardness values were measured on the matrix.

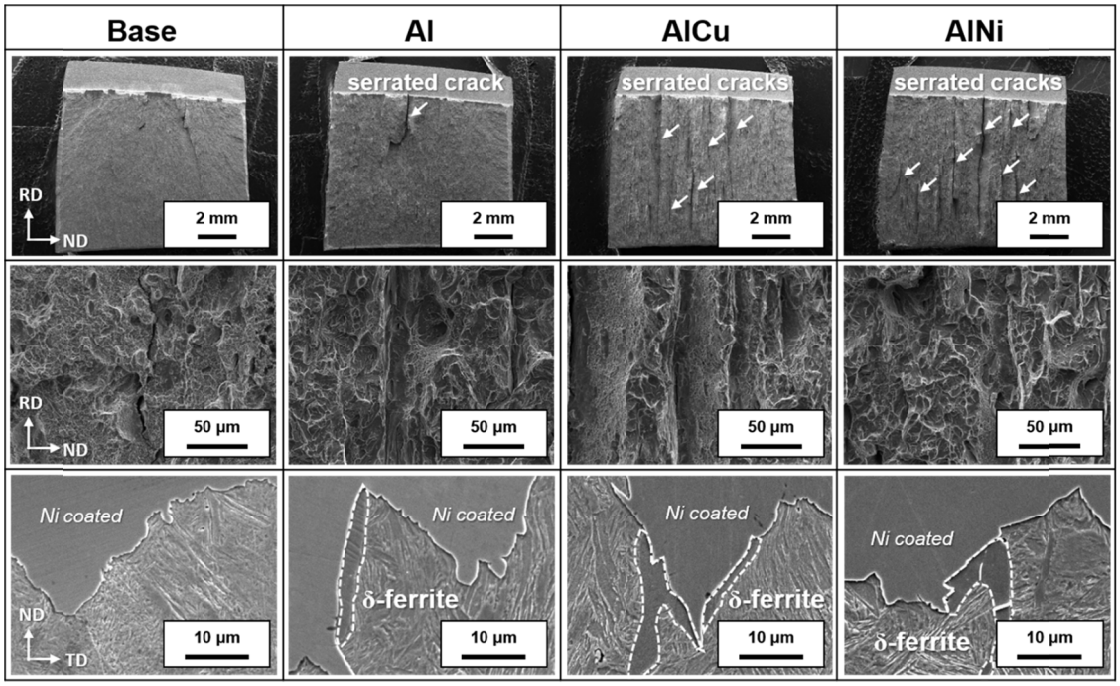

Fig. 4. SEM fractographs and the cross-sectional area of cracked regions of Charpy impact specimens for the hot-rolled Fe-9Mn-0.2C-0.5Si medium-manganese steels. The white arrows indicate the formation of cracks

The SEM fractograph and cross-sectional area of the specimens after Charpy impact tests are presented in Fig. 4. Low-magnification fractographs of the Al, AlCu, and AlNi steels exhibit serrated cracks indicated by the white arrows. The serrated cracks were more often found with increasing the fraction of delta-ferrite. The BASE steel had mostly a ductile-fractured surface showing fine dimples. Some portions of the fracture surface exhibited quasi-cleavage appearance caused by rapid crack propagation through strain-induced martensite [19]. To examine the propagation of cracks with the serrated cracks, the surfaces of the Al, AlCu, and AlNi steels were observed from the cross-sectional direction using SEM (Fig. 4), and the white dotted lines are the grain boundaries of the delta-ferrite grains. The SEM fractographs clearly revealed that a crack had propagated along the interface between matrix and delta-ferrite.

4. Conclusions

Based on the present investigation of the microstructures and mechanical properties of Fe-9.0Mn-0.2C medium-manganese steels with different Al, Cu, and Ni contents, the following conclusions can be drawn.

1. The microstructures of hot-rolled medium-manganese steels were composed of lath-type ferrite and martensite phases even upon air-cooling due to the high hardenability resulting from 9.0 wt.% Mn. In the medium-manganese steels containing Al, Cu, and Ni, some delta-ferrites were formed with the rolling direction and their fraction varied depending on the alloy element.
2. The tensile and Charpy impact test results indicated that the sole addition of Al reduced largely impact toughness by the presence of delta-ferrite and the decrease of austenite stability although it increased yield strength. However, the combined addition of Al and Cu or Ni showed the best combination of high yield strength and good impact toughness.
3. According to the SEM fractography analysis of post-Charpy impact test specimens, serrated cracks, and quasi-cleavage features were often found along the crack propagation direction. The separation cracks observed in cross-sectional areas were propagated along the interface between matrix and delta-ferrite.

Acknowledgments

The present study was supported by the Basic Science Research Program (NRF-2017R1A2B2009336) funded by the National Research Foundation of Korea.

REFERENCES

[1] S.I. Lee, S.Y. Lee, J. Han, B. Hwang, Mater. Sci. Eng. A **742**, 334-343 (2019).

[2] S.I. Lee, S.Y. Lee, S.G. Lee, H.G. Jung, B. Hwang, Met. Mater. Int. **24**, 1221-1231 (2018).

[3] S.Y. Lee, S.I. Lee, B. Hwang, Mater. Sci. Eng. A. **711**, 22-28 (2018).

[4] S.I. Lee, J. Lee, B. Hwang, Mater. Sci. Eng. A. **758**, 56-59 (2019).

[5] H. Gwon, S. Shin, J. Jeon, T. Song, S. Kim, B.C.D. Cooman, Met. Mater. Int. **25**, 594-605 (2019).
[6] Y. Kwon, J.H. Hwang, H.C. Choi, T.T.T. Trang, B. Kim, A. Zargaran, N.J. Kim, Met. Mater. Int. **26**, 75-82 (2020).
[7] M. Kuzmina, D. Ponge, D. Raabe, Acta Mater. **86**, 182-192 (2015).
[8] H. Choi, S. Lee, J. Lee, F. Barlat, B.C.D. Cooman, Mater. Sci. Eng. A **687**, 200-210 (2017).
[9] Z.H. Cai, H. Ding, R.D.K. Misra, H. Kong, H.Y. Wu, Mater. Sci. Eng. A **595**, 86-91 (2014).
[10] Z.C. Li, H. Ding, Z.H. Cai, Mater. Sci. Eng. A **639**, 559-566 (2015).
[11] T.W. Hong, S.I. Lee, J.H. Shim, J. Lee, M.G. Lee, B. Hwang, Korean J. Mater. Res. **28**, 570-577 (2018).
[12] M.T. Kim, T.M. Park, K.H. Baik, W.S. Choi, P.P. Choi, J. Han, Acta. Mater. **164**, 122-134 (2019).
[13] M. Soleimani, H. Mirzadeh, C. Dehghanian, Met. Mater. Int. **26**, 882-890 (2020).
[14] S. H. Kim, H. Kim, N. J. Kim, Nature **518**, 77-19 (2015).
[15] J.H. Hollomon, Trans. Metall. Soc. AIME, **162**, 268-290 (1945).
[16] G E. Dieter, McGraw-Hill, Mechanical Metallurgy, London 1988.
[17] J. Chen, M. Lv, S. Tang, Z. Liu, G. Wang, Mater. Charact. **106**, 108-111 (2015).
[18] Y.K. Lee, J. Han, Mater. Sci, Technol. **31**, 843-856 (2015).
[19] J. Han, A.K. Silva, D. Ponge, D. Raabe, S.M. Lee, Y.K. Lee, S.I. Lee, B. Hwang, Acta Mater. **122**, 199-206 (2017).